HHS Public Access

Author manuscript

*Oncogene*. Author manuscript; available in PMC 2015 October 09.

Published in final edited form as:

*Oncogene*. 2015 April 9; 34(15): 1979–1990. doi:10.1038/onc.2014.123.

# Vimentin regulates lung cancer cell adhesion through a VAV2-Rac1 pathway to control focal adhesion kinase activity

**Lauren S. Havel**[1], **Erik R. Kline**[1], **Alessandra M. Salgueiro**[1], and **Adam I. Marcus**[1]

[1]Emory University Winship Cancer Institute, Department of Hematology and Medical Oncology

## Abstract

Vimentin is an intermediate filament protein whose expression correlates with increased metastatic disease, reduced patient survival, and poor prognosis across multiple tumor types. Despite these well-characterized correlations, the molecular role of vimentin in cancer cell motility remains undefined. To approach this, we used an unbiased phosphoproteomics screen in lung cancer cell lines to discover cell motility proteins that show significant changes in phosphorylation upon vimentin depletion. We identified the guanine nucleotide exchange factor (GEF) VAV2 as having the greatest loss of phosphorylation due to vimentin depletion. Since VAV2 serves as a GEF for the small Rho GTPase Rac1, a key player in cell motility and adhesion, we explored the vimentin-VAV2 pathway as a potential novel regulator of lung cancer cell motility. We show that VAV2 localizes to vimentin positive focal adhesions (FAs) in lung cancer cells and complexes with vimentin and focal adhesion kinase (FAK). Vimentin loss impairs both pY142-VAV2 and downstream pY397-FAK activity showing that vimentin is critical for maintaining VAV2 and FAK activity. Importantly, vimentin depletion reduces the activity of the VAV2 target, Rac1, and a constitutively active Rac1 rescues defects in FAK and cell adhesion when vimentin or VAV2 is compromised. Based upon this data, we propose a model whereby vimentin promotes FAK stabilization through VAV2-mediated Rac1 activation. This model may explain why vimentin expressing metastatic lung cancer cells are more motile and invasive.

### Keywords

Cell Adhesion; Vimentin; Cell motility; FAK; Focal Adhesion

## Introduction

Lung cancer is the leading cause of cancer death in the United States [1]. Non-small cell lung cancer (NSCLC), in particular, accounts for about 80% of lung cancer deaths [2] and has a 5-year survival rate of only 15–25% [3]. The poor survival rate results from frequent diagnosis at advanced stages of the disease when metastasis of the primary tumor has already occurred [2].



Address correspondence to: Adam Marcus, 1365C Clifton Rd NE Room C4092, Atlanta, GA 30322., aimarcu@emory.edu, Phone Number: 404-778-4597, Fax Number: 404-778-5530.

The authors declare no conflict of interest.

Metastasis is initiated by genetic and epigenetic factors, leading to the transformation of stationary epithelial cells to migratory cells [4, 5]. This transition, called epithelial mesenchymal transition (EMT) [6, 7], is characterized by cell morphology alterations, cytoskeletal reorganization, protein expression changes, enhanced cell adhesion to the extracellular matrix (ECM), cell-cell adhesion loss, and cell polarity loss [8]. A well-characterized biomarker of EMT is the intermediate filament vimentin. Numerous publications across multiple tumor types show that it is specifically expressed in invasive cell lines and aggressive epithelial-derived tumors, but not expressed in stationary cells [9–16]. Furthermore, vimentin expression correlates with increased metastasis, reduced survival and poor prognosis for NSCLC patients [17–19]. Despite this clinical correlation, the precise molecular role of vimentin in cancer metastasis is undefined.

Mounting evidence implicates vimentin as a regulator of focal adhesions (FAs) and motility. Vimentin assembly into focal adhesions is a critical determinant of cell adhesion strength [20] and vimentin overexpression enhances FA turnover [21]. Since vimentin enters into FA sites [22–24] and regulates cell adhesion, a potential molecular link between vimentin and focal adhesion kinase (FAK) exists; however this remains uninvestigated. This is further supported by observations that vimentin binds β1 integrin [23] and that the complex formed by FAK, Src, β1 integrin and other proteins is essential for cell migration [25, 26]. Taken together, vimentin has been implicated in cell motility, invasion [27, 28], and lamellipodia formation [29]. While these studies link vimentin expression and function to cell adhesion and migration, the precise mechanisms remain elusive.

Here we identify a novel vimentin-dependent mechanism for cell adhesion and motility. We identified VAV2, a Rac1 guanine nucleotide exchange factor (GEF), whose phosphorylation at Y142 is dependent upon vimentin expression. We use this information to test a vimentin-based model of lung cancer cell adhesion and motility, whereby vimentin promotes VAV2-mediated Rac1 activation at focal adhesions, leading to stabilization of FAK positive FAs through a potential feedback loop. These data provide a new role for vimentin in mediating lung cancer cell adhesion. Since the initiation of metastasis is accompanied by changes in cell adhesion and motility, these findings may provide insight into the mechanisms driving lung cancer metastasis.

## Results

### Vimentin regulates lung cancer cell migration, invasion and metastasis

Vimentin expression is well correlated with increased cell motility and invasiveness; however, to verify this correlation in lung cancer cells, H1299 lung cancer cells were transfected with vimentin siRNA (Fig. S1A). Vimentin-depleted cells showed less cell motility in a wound-healing assay (Fig. S1B) and significantly less invasion in a standard Matrigel Boyden chamber assay (Fig. S1C) compared to control siRNA-transfected cells.

These studies were moved into a xenograft model to determine how vimentin impacts *in vivo* metastasis. To do this, H460 lung cancer cells stably expressing vimentin shRNA (shVIM) and isogenic vector-only (pLKO.1) control cells were generated (Figure S2A). H460 shVIM cells were significantly less invasive in an *in vitro* Matrigel assay compared to

pLKO.1 cells (Fig. S2B). Cell lines were injected subcutaneously in the flank of nude mice. The primary tumor volume was not significantly different between the control pLKO.1 and H460 shVIM groups (Fig. S2C); however, there was a significant difference in the number of metastatic lung nodules in the H460 shVIM xenograft compared to control (Fig. S2D, E). Furthermore, H460 shVIM-injected mice had significantly fewer micrometastases compared to pLKO.1-injected mice (Fig. S2F, G). Together, these data show that vimentin is important for *in vitro* lung cancer cell motility and invasion, as well as *in vivo* metastasis.

## Vimentin regulates VAV2 phosphorylation and localizes VAV2 to FAs

To investigate how vimentin may regulate cell motility, we performed a phospho-proteomic screen to identify cell motility related proteins that have significant changes in phosphorylation status upon stable vimentin depletion. H460 shVIM and pLKO.1 lysates were probed with 1,318 phospho-specific antibodies and their corresponding non-phosphorylated antibodies (Fig. S3; Table S1). The ratio of phosphorylated/total protein was calculated for each screened protein. For each protein, this ratio in shVIM cells was plotted against this ratio in isogenic control H460 cells (Fig. 1A). This analysis identified the guanine nucleotide exchange factor (GEF) VAV2 as having the greatest phosphorylation decrease (at Y142) in shVIM cells compared to control. These data were then presented as percent change in phosphorylation and VAV2 showed the greatest percent decrease upon vimentin depletion (Figs. 1B–C). VAV2 is a GEF for the Rho family GTPases Rac1 and cdc42, and is implicated in cell motility, invasion and spreading [30–33]. Regulation of VAV2 activity occurs through by EGFR phosphorylation of tyrosines 142, 159 and 172 [34]. To validate these findings, western blotting of H460 and H1299 shVIM and pLKO.1 cell lines was performed. Consistent with the screen, vimentin depletion resulted in decreased VAV2 phosphorylation at Y142 in both cell lines (Fig. 1D). Additionally, pY172-VAV2 levels also decreased in vimentin depleted H1299 cells (Fig. 1E), provided further evidence that VAV2 activation is reduced upon vimentin loss. When GFP tagged vimentin (hVIM-GFP), which is under the control of a tetracycline inducible promoter, was expressed in HEK 293 cells, VAV2 Y142 phosphorylation increased (Fig. 1F). Therefore, we have identified a novel downstream GEF whose phosphorylation is dependent upon vimentin expression.

To observe pY142-VAV2 localization in both the pLKO.1 and the shVIM cells, H460 shVIM or pLKO.1 cells were co-stained for vimentin and pY142-VAV2. In pLKO.1 cells, pY142-VAV2 was localized to discrete structures near the periphery of the cell, which resemble FA sites; however, when vimentin is lost, pY142-VAV2 was nearly absent at adhesion sites and its localization became more nuclear (Fig. 2A–B). While there was no significant difference in the size or intensity of the pY142-VAV2 focal adhesion sites, the number of sites was significantly reduced upon vimentin loss (Fig. 2C). Since tyrosine 172 phosphorylation of VAV2 is one of the other residues necessary for VAV2 activity [34], we also analyzed its localization by immunocytochemistry. pY172-VAV2 also appears to be localized to the FAs of H1299 cells (Fig. S4A). Since VAV2 is phosphorylated through EGFR signaling[35], we sought to determine whether vimentin regulates EGFR-mediated VAV2 phosphorylation. We found that vimentin regulated EGFR-mediated phosphorylation of Y142-VAV2 and Y172-VAV2, since shVIM cells had reduced pY147 and pY172-VAV2 levels compared to control cells after the addition of EGF (Fig. S4B).

To examine the interaction between vimentin and VAV2, we performed a co-IP and show that pY142-VAV2 co-immunoprecipitates with vimentin in total cell lysates. (Fig. 2D). To determine if pY142-VAV2 sites were indeed FA sites, H460 cells were co-stained for pY142-VAV2 and focal adhesion kinase (FAK), which serves as a FA marker. These data showed that pY142-VAV2 co-localizes with FAK at the cell periphery (Fig. 2E) and a co-immunoprecipitation revealed that pY142-VAV2 and FAK associate (Fig. 2F). Together, these data indicate that active VAV2 is a member of the FA complex and vimentin is necessary for proper pY142-VAV2 localization to FAs.

### Vimentin loss leads to decreased FAK activation at FA sites

Since vimentin is important for proper VAV2 activity and VAV2 localizes to FAK-positive adhesion sites, we tested whether vimentin is required for proper FAK localization. pY397-FAK sites were imaged at the leading edge of motile isogenic control pLKO.1 and shVIM cells (in H1299 and H460 lung cancer cell lines). In shVIM cells, FAK sites were less numerous, smaller, and less intense than in pLKO.1 cells (Figs. 3A–F). Furthermore, total FAK staining showed a similar pattern, in which shVIM cells had reduced total FAK sites (Fig. 3G). In pLKO.1 H1299 and H460 cells, vimentin filaments and squiggles were observed that directly entered into pY397-FAK sites (Figs. 3A–B, E), suggesting a possible association between pY397-FAK and vimentin. This is consistent with previous observations that vimentin enters into adhesion sites [22–24, 36–39]. To confirm that this effect is not specific to FAK and VAV2, we co-stained H460 shVIM and pLKO.1 cells for vimentin and pY418-Src and observed a reduction in the number of pY418-Src positive FA sites (Fig. S5). Taken together, these data indicate that vimentin is important for maintaining FAK positive FAs and suggest an association between vimentin and FAK.

To further probe vimentin's effect on FAK, western blotting for pY397-FAK and total FAK in lysates from three different isogenic pairs of shVIM and pLKO.1 lung cancer cell lines was performed. In all cases, pY397-FAK and total FAK levels decreased with vimentin depletion, thereby confirming that vimentin is required for FAK activity and expression (Fig. 4A). This result was confirmed using an independent vimentin shRNA clone (Fig. 4B). Furthermore, FAK mRNA levels were unchanged in the isogenic pairs, indicating that this was likely not occurring at the transcriptional level (Fig. 4C). Since total FAK levels were reduced upon vimentin depletion, the effect of vimentin on FAK protein stability was investigated by treating H1299 shVIM and pLKO.1 cells with cycloheximide (CHX) to inhibit new protein translation. After 12 hours of CHX treatment in control cells, FAK protein was still present; however after only 2 hours in shVIM cells there was little remaining total FAK (Fig. 4D). Since FAK can be degraded by calpains, [40, 41] we investigated whether vimentin regulates calpain mediated cleavage of FAK using two calpain inhibitors. In both cases, the calpain inhibitors did not significantly suppress vimentin loss-induced FAK degradation suggesting that FAK is being degraded through an alternative degradation pathway (Fig. S6).

To determine if vimentin overexpression can increase Y397-FAK and total FAK expression, a GFP tagged vimentin (hVIM-GFP) under the control of a tetracycline-inducible promoter, was introduced into HEK 293 cells. Western blotting showed that both FAK expression and

Y397 phosphorylation increased after tetracycline induction of hVIM-GFP (Fig. 4E). These data show that vimentin overexpression can trigger increased FAK activity and protein expression, and in combination with our previous data suggests that vimentin loss leads to defects in FAK stability.

Based upon our immunofluorescence data showing that vimentin enters into FAK sites, we tested whether vimentin can interact with FAK. A co-immunoprecipitation was performed for endogenous vimentin and FAK from H1299 and an association between the two proteins was observed (Fig. 4F). Next, we hypothesized that Y397-FAK could be critical for this association since this is the initial FAK autophosphorylation site. To test this, FLAG tagged phosphomimetic (Y397E) and loss-of-phosphorylation (Y397F) FAK mutants were generated. A co-immunoprecipitation between these mutants and vimentin showed that the loss of FAK phosphorylation in the Y397F mutant caused a near complete loss of association with vimentin, while the phosphomimetic mutant still associated with vimentin (Fig. 4G). This finding shows that an intact Y397 FAK site is critical for the association of FAK with vimentin and together these data implicate vimentin as a regulator of FAK activity and stability.

## Vimentin-mediated cell adhesion is dependent on FAK activation

Since we found that vimentin regulates FAK activity, we explored how this impacts cancer cell adhesion. Cellular attachment and detachment rates of H1299 and H460 pLKO.1 cells and their shVIM isogenic counterparts were measured on fibronectin-coated surfaces. Both shVIM cell lines attached slower than the pLKO.1 cells (Fig. 5A, B) indicating attachment defects. Furthermore, both shVIM H1299 and H460 cell lines detached faster after trypsinization than the pLKO.1 cells (Fig. 5C, D). Taken together, these data suggest that shVIM cells have weakened adhesion abilities.

To determine if these adhesion defects are mediated by FAK, H1299 shVIM cells were transfected with constitutively active (CA) Y397E FAK-GFP, wild-type (WT) FAK-GFP, or GFP (Fig. S7A). Transfected FAK was expressed at a slightly higher level than endogenous FAK (Fig. S7B). After trypsin treatment, shVIM cells were less adherent as shown previously, but these defects were nearly completely rescued in WT and Y397E FAK expressing cells (Fig. 5E, F), indicating that while vimentin loss leads to cell adhesion defects, these defects can be restored by overexpressing FAK or expressing a CA-FAK.

## VAV2 regulates vimentin-dependent FAK activation and cell adhesion

Since we demonstrated that vimentin regulates both VAV2 and FAK activity and localization, and that VAV2 localizes to FAK sites, we hypothesized that vimentin regulates FAK via VAV2. To test this, we first determined whether VAV2 depletion impacts pY397-FAK. Transfection of H1299 cells with VAV2 siRNA resulted in decreased pY397-FAK levels compared to cells transfected with control siRNA, with no change in total FAK levels (Fig. 6A), suggesting that VAV2 can regulate FAK activity. We also tested the possibility that FAK impacts VAV2 phosphorylation by determining whether FAK depletion leads to decreased VAV2 phosphorylation. These data show that despite significant siRNA based

FAK depletion, there is no change in VAV2 phosphorylation at Y142 and Y172 indicating that FAK does not impact VAV2 activity directly (Fig. 6B).

To determine if a constitutively active (CA) VAV2 can rescue FAK defects in vimentin-depleted cells, a GFP tagged CA VAV2 construct in which the first 184 amino acids are deleted (CA VAV2-GF2) was used [30, 42–44]. As a negative control, a truncated GFP tagged dominant negative VAV2 mutant that consists only of the C-terminal SH3, SH2 and SH3 domains was used. Transfection of shVIM cells with CA VAV2-GFP, but not the wild-type VAV2-GFP, rescued the pY397-FAK defects seen in shVIM cells (Fig. 6C). A complementary experiment showed that active VAV2 also rescued the cell adhesion defects observed in vimentin-depleted cells (Fig. 6D). These results show that an active VAV2 rescues both pY397-FAK defects and cell adhesion defects in vimentin-depleted cells.

### Vimentin regulates VAV2-mediated Rac1 activation

Since VAV2 is a GEF for the small Rho GTPases Rac1 and cdc42 [30, 32, 42], we tested whether VAV2 acts through Rac1 and/or cdc42 to regulate FAK. In control and shVIM cells, Rac1 activity had a partial but significant decrease in activity upon vimentin depletion (Fig. 7A). Importantly, CA VAV2, but not dominant negative or wild-type VAV2, could rescue Rac1 activity defects in vimentin-depleted cells (Fig. 7B), indicating that activating VAV2 can bypass vimentin function. VAV2 is also a GEF for the small rhoGTPase cdc42; however cdc42 activity was not significantly reduced in shVIM cells compared to control cells (Fig. S8A), suggesting that vimentin regulates Rac1 but not cdc42 activity in lung cancer cells.

Next, we tested whether a CA Q61L Rac1 can rescue pY397-FAK levels in vimentin-depleted cells. H1299 shVIM cells were transfected with the Q61L Rac1 active mutant, T17N Rac1 inactive mutant or WT Rac1[45] and pY397-FAK levels were assessed by western blotting. Q61L Rac1, but not WT or T17N Rac1, could rescue pY397-FAK levels (Fig. 7C; a similar experiment was also done with cdc42 but a rescue was not observed, Fig S8B). Along the same lines, confocal imaging was done to test whether expression of the Q61L Rac1 mutant in shVIM cells led to an increase in the number of Y397-FAK sites at the cellular leading edge (Fig. 7D). These data show that CA Q61L Rac1 can induce focal adhesion site formation and restore vimentin defects in cell adhesion, which is consistent with the data shown in Fig 7C. Lastly, we tested whether defects in Rac1 activity would be observed during cell spreading. To do this, serum starved H1299 shVIM and pLKO.1 cells were trypsinized then replated in serum containing media. Peak Rac1 activity was observed at 2 hrs in pLKO.1 control cells but shVIM cells lacked any observable Rac1 peak (Fig. 7E), suggesting that Rac1 defects are also observed during cell spreading. Taken together, these data further support the model that vimentin signals through VAV2-Rac1 to regulate FAK based cell adhesion.

## Discussion

Though vimentin has been repeatedly shown to correlate with metastatic disease and cell motility [10–14, 19], it has been severely understudied as a key regulator of cell motility. Unlike actin and microtubules, which rarely change total expression levels, vimentin is uniquely

expressed in invasive cancer cells and other motile cells. Here we describe a novel mechanism for vimentin-dependent lung cancer cell adhesion. We show that vimentin is required for FAK activity and localization at the cellular leading edge of motile lung cancer cells (Figs. 3, 4). We propose that vimentin regulates FAK via a VAV2-Rac1 pathway (Fig. 8) based upon three lines of evidence. First, vimentin depletion causes reduced VAV2 and Y397-FAK expression, and reduced Rac1 activity. These vimentin-associated defects, along with weakened adhesion, can be rescued with a CA VAV2, showing that VAV2 lies upstream of FAK and Rac1 activity. Interestingly, the dominant negative VAV2 also showed a rescue of pY397-FAK levels but to lesser extent than CA VAV2, which could perhaps be due to incomplete inactivation of VAV2 activity. Second, vimentin is essential for proper VAV2 localization to FAK-positive adhesion sites and VAV2 associates with vimentin and FAK. We believe that this occurs at adhesion sites, since vimentin directly enters VAV2 and FAK adhesion sites. Interestingly, the FAK Y397 autophosphorylation site appears to be critical for its association with vimentin, since when abolished, the association between FAK and vimentin is lost. Third, CA Rac1 can rescue FAK defects observed in vimentin-depleted cells, which includes restoring Y397-pFAK levels and localization at the cellular leading edge. Based upon these data, we propose a model in which vimentin is required for proper VAV2 localization to FAs, where VAV2 serves as a Rac1 GEF, and active Rac1 then promotes FAK-positive FA assembly (Fig. 8). This is consistent with previous reports showing that Rac1 regulates FAs [46–49]. Thus, vimentin promotes FA assembly through VAV2-Rac1. Since changes in cell adhesion accompany cell motility, this model provides insight into the mechanism of cell motility.

This model is consistent with the findings of other groups showing that FAs containing vimentin are larger and more stable [22, 39], and that adhesions are weaker when vimentin is absent [24]. One could speculate that when vimentin is expressed, VAV2 is actively phosphorylated and hence Rac1 activated. It was previously shown that VAV2 regulates cell invasion and spreading [32, 33] and its activation is linked to cancer invasion and metastasis [32, 50]. VAV2 activation is regulated by EGFR phosphorylation at tyrosines 142, 159 and 172, which is suggested to regulate protein interactions with VAV2 [34] to control VAV2 activity. VAV2 and the family member VAV3 are necessary for breast cancer metastasis to the lung. VAV2 and VAV3 knockdown reduced both primary tumorigenesis and lung metastasis. Furthermore, VAV2 and VAV3 overexpression in non-metastatic cells induced metastasis from the primary tumor to the lung [50].

The modest decrease in Rac1 activity upon vimentin depletion in stably adherent cells is likely explained by the fact that VAV2 is one of many GEFs for Rac1[51–53]. The remaining Rac1 activity after vimentin depletion could potentially be due to other Rac1 GEFs. Interestingly, Rac1 but not cdc42 activity is dependent upon vimentin expression. VAV2 is a Rac1 GEF [30, 32, 54] though its role as a cdc42 GEF remains controversial [44]. Rac1 is targeted to FAs and is required for FA complex assembly [46, 52]. Therefore, we believe that the reduced Rac1 activity results in reduced FAK phosphorylation and improper FAK localization. This is based upon our data showing that a CA Rac1 can rescue vimentin defects and restore normal FAK phosphorylation and localization. Since other groups have shown that pFAK is necessary for Rac1 activation[52, 55, 56], and another group has more specifically found that FAK mediates Rac1 targeting to FAs through tyrosine

phosphorylation of the GEF, βPIX [52], we propose a potential feedback loop between Rac1 and FAK, where increased FAK activity can in turn activate Rac1; however, we do not believe this is through VAV2 since VAV2 activity is unaffected by FAK depletion (Fig 6B).

Taken together, the work presented here identifies vimentin as a regulator of FA architecture and signaling through VAV2-Rac1 signaling. Since proper functioning of the FAs is required for cell motility and metastasis, this work could lay the groundwork for future studies examining the downstream molecular consequences of vimentin targeting in lung cancer.

## Materials and Methods

### Cell Culture

H1299, H460 and H1792 cell lines were grown in RPMI 1640 media supplemented with 10% FBS and 1% penicillin/streptomycin and maintained in a humidified chamber at 37 °C with 5% $CO_2$. HEK 293 cells were grown in DMEM media supplemented with 10% FBS and 1% penicillin/streptomycin. All tissue culture plates and coverslips used for experiments were covered with 5 μg/cm$^2$ human plasma fibronectin (Millipore) diluted in PBS and incubated for 30 min at 37 °C prior to cell seeding.

### Antibodies

Antibodies against pY397-FAK (Invitrogen), FAK (BD Biosciences), GAPDH (Cell Signalling), vimentin (Sigma), pY142-VAV2 (Full Moon Biosystems), pY172-VAV2 (Abcam), VAV2 (Full Moon Biosystems), GFP (Covance, Princeton, NJ), pY418-Src (Invitrogen) and FLAG (Sigma) were used for Western blotting, immunofluorescence and immunoprecipitation. HRP-conjugated secondary antibodies (Jackson ImmunoResearch) were used for Western blotting.

### Transfections and Drug Treatments

Lipofectamine 2000 and Plus reagents (Invitrogen) were used to transfect the FLAG, WT FAK-FLAG, Y397E FAK-FLAG, Y397F FAK-FLAG, GFP, WT FAK-GFP, Y397E FAK-GFP, WT VAV2-GFP, CA VAV2-GFP, inactive VAV2-GFP, WT Rac1-GFP, Q61L Rac1-GFP, T17N Rac1-GFP, WT cdc42-GFP, Q61L cdc42-GFP and T17N cdc42-GFP constructs according to the Invitrogen supplied protocol. The RevTet-On system (Clontech), which includes pRevTRE carrying the human vimentin gene and pRevTet-On, was used. Oligofectamine (Invitrogen) was used to transiently transfect cells with VAV2 small interfering RNA (siRNA) (Qiagen FlexiTube VAV2 6. Cat. No. SI02662947), vimentin siRNA (Qiagen FlexiTube Hs_VIM_13. Cat. No. SI04201890) or FAK siRNA (ThermoScientific ON-TARGET plus PTK2 Cat. No. L-003164-00-0005) according to the manufacturer's protocol. Two successive 24-hour transfections were performed before cell harvesting. For the production of stable vimentin knock-down H1299, H460 and H1792 lung cancer cells, vimentin shRNA (ThermoScientific, Catalog No. RHS3979-201759429, clone ID TRCN0000029122) and shVIM clone 2 were (ThermoScientific, Catalog No. RHS3979-201759427, clone ID TRCN0000029119) delivered in pLKO.1 lentiviral vectors (ThermoScientific). The shVIM sequence is 5′-TTGAACTCGGTGTTGATGGCG-3′ and

the shVIM clone 2 sequence is 5′-AATAGTGTCTTGGTAGTTAGC-3′. To produce the virus, HEK 293T cells were transfected with the shRNA and helper plasmids (pHRCMV8.2ΔR and CMV-VSVG) using LT1 transfection reagent (Myrius). To harvest the lentiviral stock, the media was centrifuged at 250g for 5 min then filtered through a syringe. Cells were infected with a 1:4 dilution of lentivirus in complete media containing 8 μg/mL polybrene. The next day, the media was changed to complete media containing 2 μg/mL puromycin. For the cyclohexamide (CHX) experiment, H1299 cells were treated with 20 ug/mL cyclohexamide (Sigma) in complete RPMI media.

## Adhesion assays

For the detachment assays, cells were plated at $1 \times 10^5$ or $1.5 \times 10^5$ cells/well of a 12-well plate, respectively. After 24 hours, each well was trypsinized for lengths of time ranging from 0 to 5 min. At each time point, 2 times the trypsin volume of complete RPMI media was added to the well. The non-adherent cell containing media was aspirated off and each well was washed with 1X PBS. The remaining adherent cells were trypsinized and counted. The number of adherent cells in each well was normalized to the total number of cells (0 time point). For the attachment assays, the concentration of each cell line after collection by trypsinization was equalized to $5 \times 10^5$ cells/mL. 1 mL of cells was added to each well of a 12-well plate and incubated for varying lengths of time ranging from 10 to 90 min. At each time point, the non-adherent cells were aspirated off. The adherent cells were washed gently with PBS, trypsinized then counted.

## Western Blotting

Cells were harvested and lysed in cold TNES buffer (50 mM Tris pH 7.5, 100 mM NaCl, 2 mM EDTA, 1% Nonidet P-40, 1X Roche Complete Protease Inhibitors, 10 mM NaF, 1 mM $NaVO_4$, 2 mM sodium pyrophosphate, and 2 mM β-glycerophosphate). Protein concentrations were determined using a protein assay kit (Pierce). Equal protein concentrations of whole cell lysate were solubilized in SDS sample buffer, separated on a 10% SDS-polyacrylamide gel, and transferred to a methanol soaked polyvinyalide diflouride (PVDF) membrane, which was then blocked with 10% milk in 1X TBST. Primary antibody, diluted in 5% milk in TBST, was added to the membrane while rocking overnight at 4°C. After 3 TBST washes, the appropriate HRP conjugated secondary antibody diluted in 5% milk in TBST was added to the blot for 1 h at room temperature. After 3 more TBST washes, proteins were visualized using a chemiluminescent substrate (Denville).

## Quantitative Real-Time PCR

Total RNA was isolated using an RNeasy Mini Kit (Qiagen) then reverse transcribed with M-MLV Reverse Transcriptase (Invitrogen). The cDNA product was amplified using sequence specific primers to FAK (forward- TGGTGAAAGCTGTCATCGAG, reverse-TCATCCACAGTGGCCAATAA) and analyzed by real-time PCR using SYBR green detection. 25μL reactions contained 1 μL DNA, 0.2 μM of each primer, and 12.5 μL IQ SYBR Green Supermix (Bio-Rad). The following PCR protocol was used: 3 min hot start at 95 °C followed by cycles of 95 °C, 10 s; 55 °C 60 s. Melt curve analysis verified a single product. Relative RNA quantities were calculated then standardized to levels of 18S rRNA.

### Immunofluorescence

Cells were fixed on 1.5mm glass coverslips with PHEMO buffer (68 mM, PIPES, 25 mM HEPES, 15 mM EGTA, 3 mM $MgCl_2$, 10% DMSO) plus 3.7% formaldehyde, 0.05% glutaraldehyde and 0.5% Triton X-100 for 10 min at room temperature. After three 5 min washes with PBS, the coverslips were blocked with 10% normal goat serum for 1 h at room temperature. Primary antibodies were diluted in 5% normal goat serum and added to the coverslips overnight at 4 °C. After 3 PBS washes, the coverslips were incubated for 1 h at room temperature with a fluorophore conjugated secondary antibody diluted in 5% normal goat serum. After 3 PBS washes, the coverslips were incubated with 350 nM DAPI stain diluted in 1X PBS for 10 min at room temperature. The coverslips were mounted on glass slides using Prolong gold mounting medium (Invitrogen). The slides were imaged using Zeiss LSM 510 META confocal microscope using a 100X oil Plan-Apo objective (NA = 1.46). The images were processed using ZEN 2009 software. A Nikon N-SIM microscope housed within the Emory Integrated Cellular Imaging Core was utilized to acquire super-resolution images of vimentin directly entering FAs. Images were acquired using a 100× 1.49 NA oil objective. All images within an experiment were taken under identical settings. Intensity levels were adjusted equally on all samples within an experiment.

### Immunofluorescence Image Quantification

To assess focal adhesion site size and intensity, images were analyzed in ImageJ/Fiji. A 100 $micron^2$ rectangle was used as a region of interest (ROI) at the leading edge of cells. Pixels within this ROI were then thresholded to remove background and the same threshold was used for all samples stained with the same antibody. The “Analyze Particle” function was then implemented to detect objects. All objects less than 0.5micrometers were then removed using a size filter. The intensities and size of the remaining objects were then quantified and imported into Excel.

### Co-immunoprecipitation

Cells were harvested and lysed in NP-40 lysis buffer (50 mM Tris pH 7.4, 50 mM NaCl, 0.1% Triton X-100, 1% NP-40) plus 1X Roche Complete Protease Inhibitors, 10 mM NaF, 1 mM $NaVO_4$, 2 mM sodium pyrophosphate and 2 mM β-glycerophosphate. For co-immunoprecipitations involving vimentin, total lysate was used. For all other co-immunoprecipitations, lysate was centrifuged at 14,000 × g at 4 °C for 10 min. 10 μg of primary antibody was incubated with 500 μg of protein at 4° C overnight while rotating. Each sample was incubated with 50 μL of Dynabeads (Invitrogen) for 1 hour at 4° C while rotating. After three 20 min washes with NP-40 lysis buffer, the protein-antibody complex was eluted from the beads in 2X Laemmli buffer at 100 °C for 10 min.

### Phosphorylation screen

H460 pLKO.1 and shVIM cell lysates were analyzed using the Phospho Explorer Antibody Array (Full Moon Biosystems), which is a microarray containing 1,318 phospho-specific antibodies spotted on a coated glass slide in duplicate. Cell lysates were given to Full Moon Biosystems for processing and analysis. Lysates were labeled with biotin then bound to the array’s antibodies. The phosphorylated protein in each sample was detected using Cy3-

streptavidin. The array was scanned with an Axon GenePix scanner to measure phosphorylation levels of individual proteins in each sample. The ratio of phosphorylated to total protein was calculated for both pLKO.1 and shVIM cells and reported as a fold change upon vimentin loss. The percent change in phosphorylation upon vimentin depletion was calculated as a ratio of phosphorylated:total protein in shVIM cells to phosphorylated:total protein in pLKO.1 cells.

### Rac1 activation assays

The G-LISA rac1 luminescence-based activation assay kit (Cytoskeleton, Denver, CO) was used to measure rac1 activity in stably adherent cells. The cells were lysed in the supplied lysis buffer. Lysates were diluted to 1 ug/uL then processed according the supplied protocol. Readings were obtained using spectraMax luminometer. For the timecourse experiment on trypsinized cells that were re-plated, we used a Rac1 activation pull-down kit (Cytoskeleton, Denver, CO). Cells were lysed in the supplied lysis buffer then diluted to 1.5 μg/μL and processed according to the supplied protocol. The pull-down products were analyzed by western blotting using a Rac1 antibody from BD Biosciences.

### Statistical Analysis

P-values of significance were obtained using one- or two-way ANOVA analysis followed by a multiple comparison test. In the case of the xenograft and qRT-PCR studies, a Student's t-test was employed.

## Supplementary Material

Refer to Web version on PubMed Central for supplementary material.

## Acknowledgments

**Funding**: Lauren S Havel – Ruth L Kirschstein National Research Service Award through the NCI (1F32CA168112-01). Adam I Marcus - NCI (1R01CA1428580)

This work was supported by the National Cancer Institute (1R01CA1428580) awarded to A.I.M and through a Ruth L Kirschstein National Research Service Award (1F32CA168112-01) awarded to L.S.H. Research reported in this publication was supported in part by the Winship and Emory Integrated Cellular Imaging Core and NIH/NCI under award number P30CA138292. The content is solely the responsibility of the authors and does not necessarily represent the official views of the National Institutes of Health. We would like to thank the the Custom Cloning Core at Emory University for generating the mutant FAK constructs and Doris Powell in the laboratory of Paula Vertino for her technical assistance with the quantitative RT-PCR experiments. We would also like to thank Anthea Hammond for reviewing this manuscript. In addition, we thank Keith Burridge at the University of North Carolina for generously supplying us with the VAV2 plasmids.

## References

1. Singh GK, Miller BA, Hankey BF. Changing area socioeconomic patterns in U.S. cancer mortality, 1950–1998: Part II--Lung and colorectal cancers. J Natl Cancer Inst. 2002; 94:916–925. [PubMed: 12072545]
2. Pisters KM, Le Chevalier T. Adjuvant chemotherapy in completely resected non-small-cell lung cancer. J Clin Oncol. 2005; 23:3270–3278. [PubMed: 15886314]
3. Patz EF Jr, Swensen SJ, Herndon JE 2nd. Estimate of lung cancer mortality from low-dose spiral computed tomography screening trials: implications for current mass screening recommendations. J Clin Oncol. 2004; 22:2202–2206. [PubMed: 15169809]

4. Herman JG, Baylin SB. Gene silencing in cancer in association with promoter hypermethylation. N Engl J Med. 2003; 349:2042–2054. [PubMed: 14627790]
5. Baylin SB, Esteller M, Rountree MR, Bachman KE, Schuebel K, Herman JG. Aberrant patterns of DNA methylation, chromatin formation and gene expression in cancer. Hum Mol Genet. 2001; 10:687–692. [PubMed: 11257100]
6. Greenburg G, Hay ED. Epithelia suspended in collagen gels can lose polarity and express characteristics of migrating mesenchymal cells. J Cell Biol. 1982; 95:333–339. [PubMed: 7142291]
7. Stoker M, Perryman M. An epithelial scatter factor released by embryo fibroblasts. J Cell Sci. 1985; 77:209–223. [PubMed: 3841349]
8. Thiery JP. Epithelial-mesenchymal transitions in tumour progression. Nat Rev Cancer. 2002; 2:442–454. [PubMed: 12189386]
9. Liu LK, Jiang XY, Zhou XX, Wang DM, Song XL, Jiang HB. Upregulation of vimentin and aberrant expression of E-cadherin/beta-catenin complex in oral squamous cell carcinomas: correlation with the clinicopathological features and patient outcome. Mod Pathol. 2010; 23:213–224. [PubMed: 19915524]
10. Hu L, Lau SH, Tzang CH, et al. Association of Vimentin overexpression and hepatocellular carcinoma metastasis. Oncogene. 2004; 23:298–302. [PubMed: 14647434]
11. Wei J, Xu G, Wu M, et al. Overexpression of vimentin contributes to prostate cancer invasion and metastasis via src regulation. Anticancer Res. 2008; 28:327–334. [PubMed: 18383865]
12. Wang JW, Peng SY, Li JT, et al. Identification of metastasis-associated proteins involved in gallbladder carcinoma metastasis by proteomic analysis and functional exploration of chloride intracellular channel 1. Cancer Lett. 2009; 281:71–81. [PubMed: 19299076]
13. Singh S, Sadacharan S, Su S, Belldegrun A, Persad S, Singh G. Overexpression of vimentin: role in the invasive phenotype in an androgen-independent model of prostate cancer. Cancer Res. 2003; 63:2306–2311. [PubMed: 12727854]
14. Liu Z, Brattain MG, Appert H. Differential display of reticulocalbin in the highly invasive cell line, MDA-MB-435, versus the poorly invasive cell line, MCF-7. Biochem Biophys Res Commun. 1997; 231:283–289. [PubMed: 9070264]
15. Chang L, Goldman RD. Intermediate filaments mediate cytoskeletal crosstalk. Nat Rev Mol Cell Biol. 2004; 5:601–613. [PubMed: 15366704]
16. Zeisberg M, Neilson EG. Biomarkers for epithelial-mesenchymal transitions. J Clin Invest. 2009; 119:1429–1437. [PubMed: 19487819]
17. Soltermann A, Tischler V, Arbogast S, et al. Prognostic significance of epithelial-mesenchymal and mesenchymal-epithelial transition protein expression in non-small cell lung cancer. Clin Cancer Res. 2008; 14:7430–7437. [PubMed: 19010860]
18. Al-Saad S, Al-Shibli K, Donnem T, Persson M, Bremnes RM, Busund LT. The prognostic impact of NF-kappaB p105, vimentin, E-cadherin and Par6 expression in epithelial and stromal compartment in non-small-cell lung cancer. Br J Cancer. 2008; 99:1476–1483. [PubMed: 18854838]
19. Dauphin M, Barbe C, Lemaire S, et al. Vimentin expression predicts the occurrence of metastases in non small cell lung carcinomas. Lung Cancer. 2013
20. Li QF, Spinelli AM, Wang R, Anfinogenova Y, Singer HA, Tang DD. Critical role of vimentin phosphorylation at Ser-56 by p21-activated kinase in vimentin cytoskeleton signaling. J Biol Chem. 2006; 281:34716–34724. [PubMed: 16990256]
21. Mendez MG, Kojima S, Goldman RD. Vimentin induces changes in cell shape, motility, and adhesion during the epithelial to mesenchymal transition. FASEB J. 2010; 24:1838–1851. [PubMed: 20097873]
22. Tsuruta D, Jones JC. The vimentin cytoskeleton regulates focal contact size and adhesion of endothelial cells subjected to shear stress. J Cell Sci. 2003; 116:4977–4984. [PubMed: 14625391]
23. Kreis S, Schonfeld HJ, Melchior C, Steiner B, Kieffer N. The intermediate filament protein vimentin binds specifically to a recombinant integrin alpha2/beta1 cytoplasmic tail complex and co-localizes with native alpha2/beta1 in endothelial cell focal adhesions. Exp Cell Res. 2005; 305:110–121. [PubMed: 15777792]

24. Bhattacharya R, Gonzalez AM, Debiase PJ, et al. Recruitment of vimentin to the cell surface by beta3 integrin and plectin mediates adhesion strength. J Cell Sci. 2009; 122:1390–1400. [PubMed: 19366731]
25. White DE, Kurpios NA, Zuo D, et al. Targeted disruption of beta1-integrin in a transgenic mouse model of human breast cancer reveals an essential role in mammary tumor induction. Cancer Cell. 2004; 6:159–170. [PubMed: 15324699]
26. Sieg DJ, Hauck CR, Ilic D, et al. FAK integrates growth-factor and integrin signals to promote cell migration. Nat Cell Biol. 2000; 2:249–256. [PubMed: 10806474]
27. Zhu QS, Rosenblatt K, Huang KL, et al. Vimentin is a novel AKT1 target mediating motility and invasion. Oncogene. 2011; 30:457–470. [PubMed: 20856200]
28. Ivaska J, Vuoriluoto K, Huovinen T, Izawa I, Inagaki M, Parker PJ. PKCepsilon-mediated phosphorylation of vimentin controls integrin recycling and motility. EMBO J. 2005; 24:3834–3845. [PubMed: 16270034]
29. Helfand BT, Mendez MG, Murthy SN, et al. Vimentin organization modulates the formation of lamellipodia. Mol Biol Cell. 2011; 22:1274–1289. [PubMed: 21346197]
30. Abe K, Rossman KL, Liu B, et al. Vav2 is an activator of Cdc42, Rac1, and RhoA. J Biol Chem. 2000; 275:10141–10149. [PubMed: 10744696]
31. Miller SL, Antico G, Raghunath PN, Tomaszewski JE, Clevenger CV. Nek3 kinase regulates prolactin-mediated cytoskeletal reorganization and motility of breast cancer cells. Oncogene. 2007; 26:4668–4678. [PubMed: 17297458]
32. Lai SY, Ziober AF, Lee MN, Cohen NA, Falls EM, Ziober BL. Activated Vav2 modulates cellular invasion through Rac1 and Cdc42 in oral squamous cell carcinoma. Oral Oncol. 2008; 44:683–688. [PubMed: 17996485]
33. Marignani PA, Carpenter CL. Vav2 is required for cell spreading. J Cell Biol. 2001; 154:177–186. [PubMed: 11448999]
34. Tamas P, Solti Z, Bauer P, et al. Mechanism of epidermal growth factor regulation of Vav2, a guanine nucleotide exchange factor for Rac. J Biol Chem. 2003; 278:5163–5171. [PubMed: 12454019]
35. Ahn J, Truesdell P, Meens J, et al. Fer protein-tyrosine kinase promotes lung adenocarcinoma cell invasion and tumor metastasis. Mol Cancer Res. 2013; 11:952–963. [PubMed: 23699534]
36. Bershadsky AD, Tint IS, Svitkina TM. Association of intermediate filaments with vinculin-containing adhesion plaques of fibroblasts. Cell Motil Cytoskeleton. 1987; 8:274–283. [PubMed: 3121191]
37. Seifert GJ, Lawson D, Wiche G. Immunolocalization of the intermediate filament-associated protein plectin at focal contacts and actin stress fibers. Eur J Cell Biol. 1992; 59:138–147. [PubMed: 1468436]
38. Gonzales M, Weksler B, Tsuruta D, et al. Structure and function of a vimentin-associated matrix adhesion in endothelial cells. Mol Biol Cell. 2001; 12:85–100. [PubMed: 11160825]
39. Burgstaller G, Gregor M, Winter L, Wiche G. Keeping the vimentin network under control: cell-matrix adhesion-associated plectin 1f affects cell shape and polarity of fibroblasts. Mol Biol Cell. 2010; 21:3362–3375. [PubMed: 20702585]
40. Chan KT, Bennin DA, Huttenlocher A. Regulation of adhesion dynamics by calpain-mediated proteolysis of focal adhesion kinase (FAK). J Biol Chem. 2010; 285:11418–11426. [PubMed: 20150423]
41. Lim JA, Hwang SH, Kim MJ, Kim SS, Kim HS. N-terminal cleavage fragment of focal adhesion kinase is required to activate the survival signalling pathway in cultured myoblasts under oxidative stress. FEBS J. 2012; 279:3573–3583. [PubMed: 22809424]
42. Liu BP, Burridge K. Vav2 activates Rac1, Cdc42, and RhoA downstream from growth factor receptors but not beta1 integrins. Mol Cell Biol. 2000; 20:7160–7169. [PubMed: 10982832]
43. Schuebel KE, Bustelo XR, Nielsen DA, et al. Isolation and characterization of murine vav2, a member of the vav family of proto-oncogenes. Oncogene. 1996; 13:363–371. [PubMed: 8710375]
44. Schuebel KE, Movilla N, Rosa JL, Bustelo XR. Phosphorylation-dependent and constitutive activation of Rho proteins by wild-type and oncogenic Vav-2. EMBO J. 1998; 17:6608–6621. [PubMed: 9822605]

45. Wittmann T, Bokoch GM, Waterman-Storer CM. Regulation of leading edge microtubule and actin dynamics downstream of Rac1. J Cell Biol. 2003; 161:845–851. [PubMed: 12796474]

46. Rottner K, Hall A, Small JV. Interplay between Rac and Rho in the control of substrate contact dynamics. Curr Biol. 1999; 9:640–648. [PubMed: 10375527]

47. Deakin NO, Ballestrem C, Turner CE. Paxillin and Hic-5 interaction with vinculin is differentially regulated by Rac1 and RhoA. PLoS One. 2012; 7:e37990. [PubMed: 22629471]

48. Carr HS, Morris CA, Menon S, Song EH, Frost JA. Rac1 controls the subcellular localization of the Rho guanine nucleotide exchange factor Net1A to regulate focal adhesion formation and cell spreading. Mol Cell Biol. 2013; 33:622–634. [PubMed: 23184663]

49. Nobes CD, Hall A. Rho, rac, and cdc42 GTPases regulate the assembly of multimolecular focal complexes associated with actin stress fibers, lamellipodia, and filopodia. Cell. 1995; 81:53–62. [PubMed: 7536630]

50. Citterio C, Menacho-Marquez M, Garcia-Escudero R, et al. The rho exchange factors vav2 and vav3 control a lung metastasis-specific transcriptional program in breast cancer cells. Sci Signal. 2012; 5:ra71. [PubMed: 23033540]

51. Yamauchi J, Miyamoto Y, Tanoue A, Shooter EM, Chan JR. Ras activation of a Rac1 exchange factor, Tiam1, mediates neurotrophin-3-induced Schwann cell migration. Proc Natl Acad Sci U S A. 2005; 102:14889–14894. [PubMed: 16203995]

52. Chang F, Lemmon CA, Park D, Romer LH. FAK potentiates Rac1 activation and localization to matrix adhesion sites: a role for betaPIX. Mol Biol Cell. 2007; 18:253–264. [PubMed: 17093062]

53. Charrasse S, Comunale F, Fortier M, Portales-Casamar E, Debant A, Gauthier-Rouviere C. M-cadherin activates Rac1 GTPase through the Rho-GEF trio during myoblast fusion. Mol Biol Cell. 2007; 18:1734–1743. [PubMed: 17332503]

54. Garrett TA, Van Buul JD, Burridge K. VEGF-induced Rac1 activation in endothelial cells is regulated by the guanine nucleotide exchange factor Vav2. Exp Cell Res. 2007; 313:3285–3297. [PubMed: 17686471]

55. Kallergi G, Agelaki S, Markomanolaki H, Georgoulias V, Stournaras C. Activation of FAK/PI3K/Rac1 signaling controls actin reorganization and inhibits cell motility in human cancer cells. Cell Physiol Biochem. 2007; 20:977–986. [PubMed: 17982280]

56. Choma DP, Milano V, Pumiglia KM, DiPersio CM. Integrin alpha3beta1-dependent activation of FAK/Src regulates Rac1-mediated keratinocyte polarization on laminin-5. J Invest Dermatol. 2007; 127:31–40. [PubMed: 16917494]

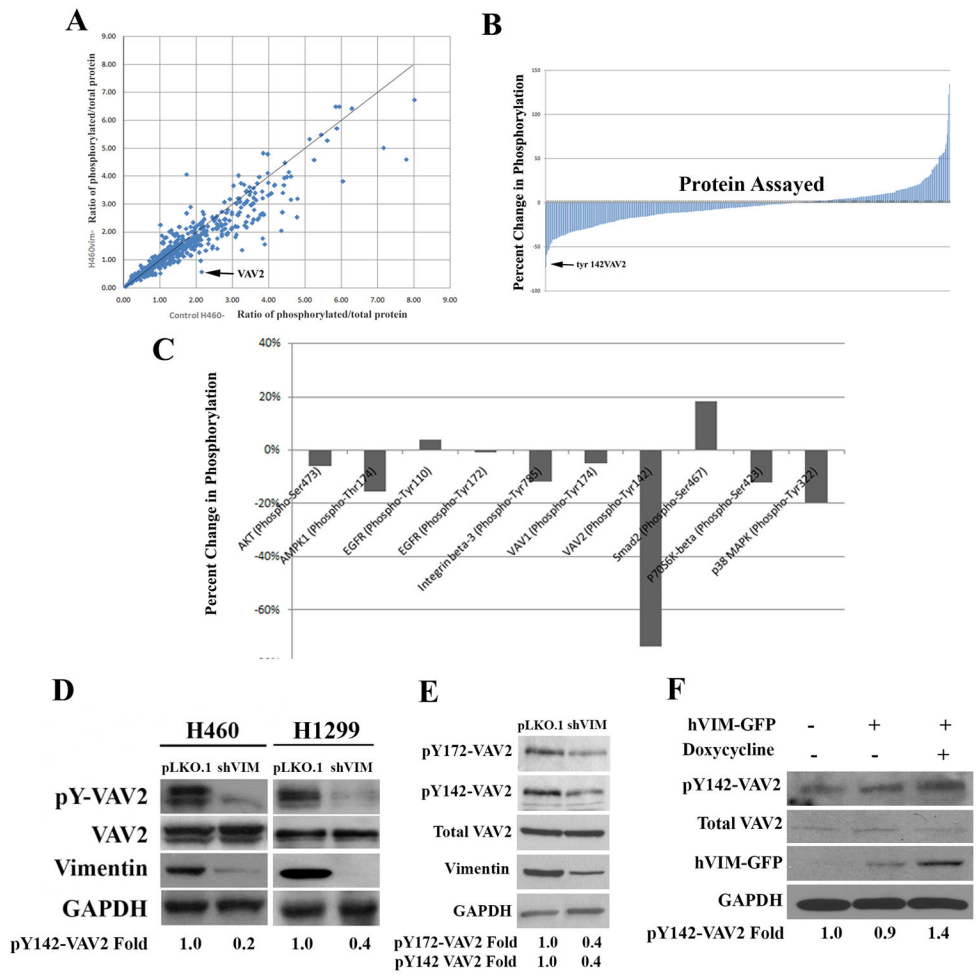


**Figure 1. Phospho-proteomic screen for cell motility proteins with an altered phosphorylation status upon vimentin depletion**

(A) For each protein analyzed, the ratio of phosphorylated/total protein in H460 shVIM cells was plotted against the same ratio in H460 pLKO.1 cells. VAV2 showed reduced phosphorylation upon vimentin loss. (B) Bar graphs showing that VAV2 had the greatest decrease in percent phosphorylation of all proteins screened. (C) Bar graph comparing VAV2 to other relevant proteins. (D) The reduction in VAV2 phosphorylation at Y142 was verified by Western blotting in H460 and H1299 cell lines. (E) Lysates from H1299 pLKO.1 or shVIM cells were analyzed by western blotting for pY172-VAV2 levels. pY172-VAV2 levels are decreased in shVIM cells. (F) Western blotting of lysate from HEK 293 cells transfected with hVIM-GFP shows a 40% increase in pY142-VAV2 upon induction of vimentin expression with doxycycline. A representative western blot out of multiple independent experiments is shown. Fold changes were determined by densitometry.

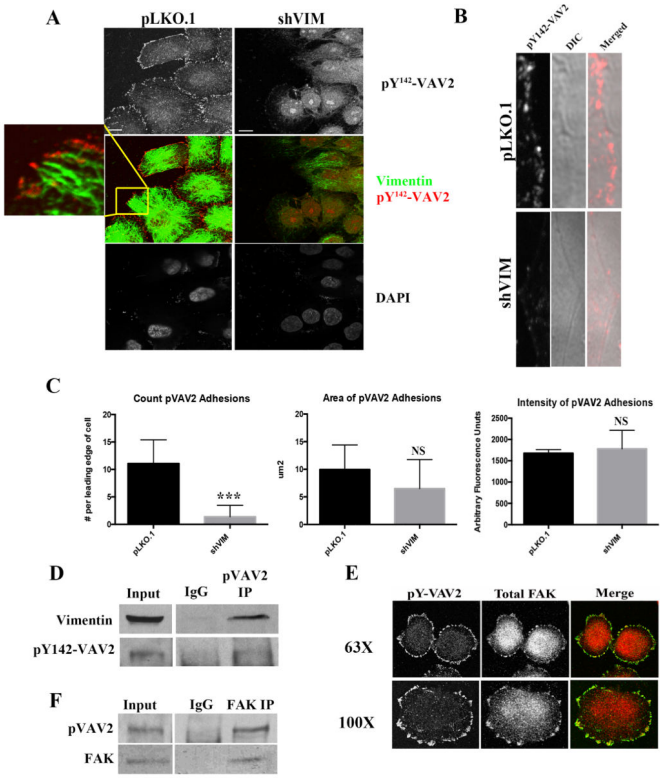


**Figure 2. pY142-VAV2 localizes to focal adhesions in vimentin positive cells**

(A) H460 pLKO.1 and shVIM lung cancer cells were co-stained for pY142-VAV2 (red) and vimentin (green). The control cells showed localization of pY142-VAV2 to focal adhesions and vimentin filaments directly entering pY142-VAV2 positive focal adhesion sites. Scale bars=10 μm. (B) H1299 pLKO.1 and shVIM cells were stained for pY142-VAV2). Images of only the cellular leading edge show the presence of pY142-VAV2 positive focal adhesion sites in the control pLKO.1 cells but not the shVIM cells. (C) Upon the loss of vimentin, there is a reduction in the number but not intensity or size of pVAV2 positive focal adhesions. (D) Co-immunoprecipitation showed an association between endogenous pY142-VAV2 and vimentin in H460 total cell lysates. IgG is shown as a negative control. (E) Confocal immunofluorescence images of H460 cells co-stained for pY142-VAV2 (green) and FAK (red). (F) Co-immunoprecipitation of endogenous pVAV2 and FAK revealed an association. IgG is shown as a negative control.

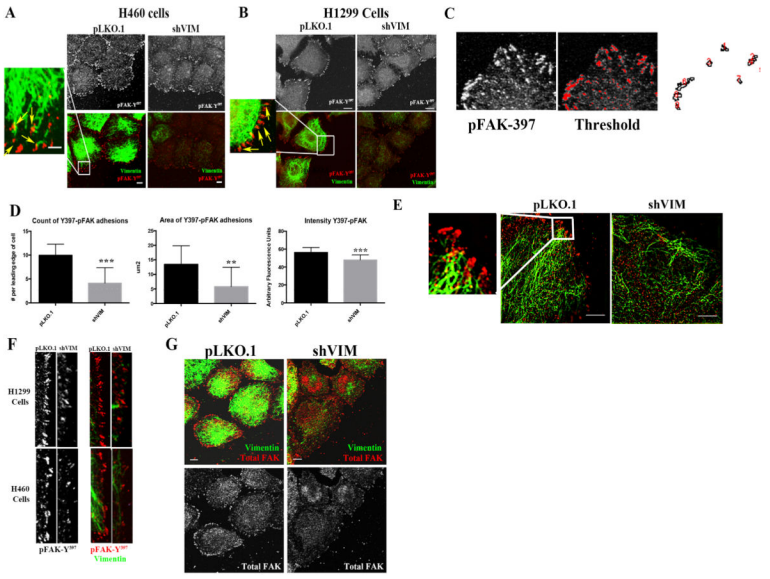


**Figure 3. Vimentin depletion reduces the number and intensity of activated FAK positive focal adhesion sites**

(A and B) Confocal immunofluorescence images of pY397-FAK (red) and vimentin (green) in H460 and H1299 cells from a wounding assay. Yellow arrows indicate where the vimentin filaments and squiggles enter the pY397-FAK sites. Scale bar = 10 μm. (C) The ROI at the leading edge of the cells, whose pixels were thresholded to remove background. (D) There is a reduction in the number, size and intensity of focal adhesions in H460 cells upon vimentin depleteion. (E) H460 cells were co-stained for pY397-FAK (red) and vimentin (green). N-SIM super resolution microscopy was used to visualize the vimentin filaments directly entering the FAK sites. Scale bar = 10 μm (F) H460 and H1299 pLKO.1 or shVIM cells were co-stained for pY397-FAK (red) and vimentin (green). Images of only the cellular leading edge show that in shVIM cells the pY397-FAK positive focal adhesion sites were less intense and less numerous. (G) H460 shVIM cells co-stained for vimentin (green) and total FAK (red) showed reduced FAK positive focal adhesions compared to H460 pLKO.1 cells. Scale bar = 10 μm.

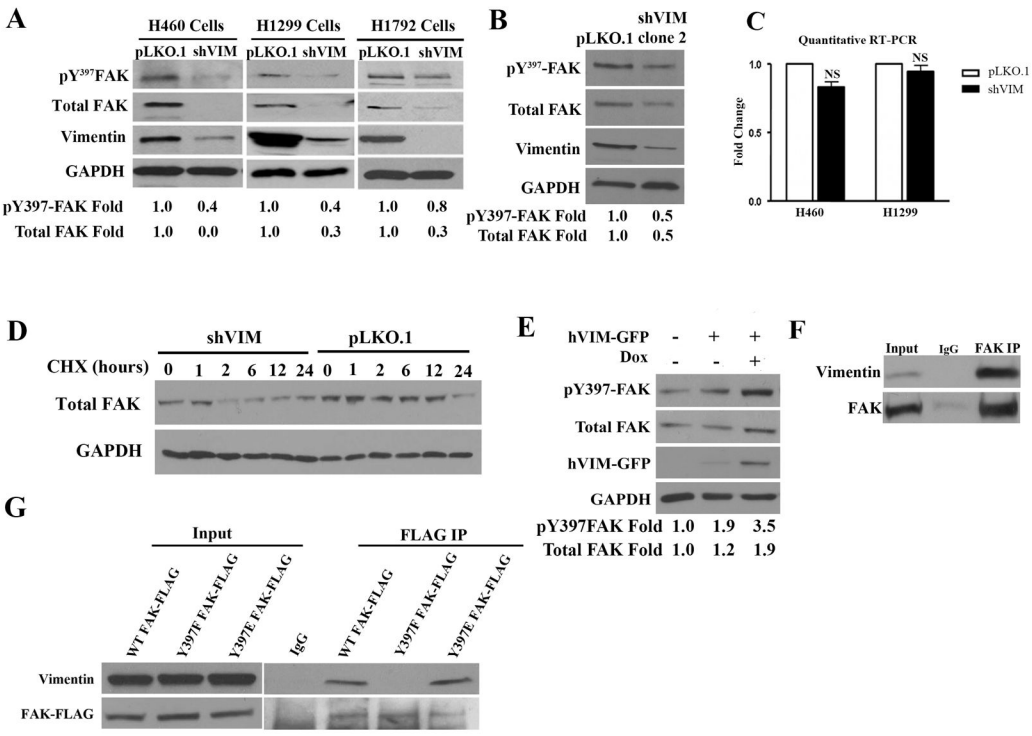


**Figure 4. Vimentin regulates FAK activation and expression**

(A) Lysates from H460, H1299 and H1792 shVIM and pLKO.1 lung cancer cell lines were analyzed by Western blotting and showed a reduction in FAK Y397 phosphorylation and expression upon vimentin depletion. A representative western blot out of multiple independent experiments is shown. Fold changes were determined by densitometry. (B) Lysates from H1299 pLKO.1 and shVIM clone 2 cells were analyzed by Western blotting for FAK expression and Y397 phosphorylation levels. (C) Quantitative real-time PCR analysis of FAK mRNA levels in H460 and H1299 shVIM and pLKO1 cells showed no significant difference. (D) H1299 shVIM and pLKO.1 cells treated with CHX were analyzed by Western blotting for total FAK levels. In the absence of vimentin, FAK levels decreased at a faster rate than in the presence of vimentin. (E) Lysates from HEK 293 cells transfected with hVIM-GFP were analyzed by Western Blotting. FAK expression and Y397 phosphorylation increased upon induction of hVIM-GFP expression with doxycycline. A representative western blot out of multiple independent experiments is shown. Fold changes were determined by densitometry. (F) Co-immunoprecipitation showed an association between endogenous FAK and vimentin in H1299 total cell lysates. IgG is shown as a negative control. (G) Lysates from H1299 cells transfected with WT FAK-FLAG, Y397F FAK-FLAG or Y397E FAK-FLAG were used for immunoprecipitation between transiently expressed FAK and endogenous vimentin. Both WT and Y397E FAK associated with vimentin whereas Y397F FAK did not.

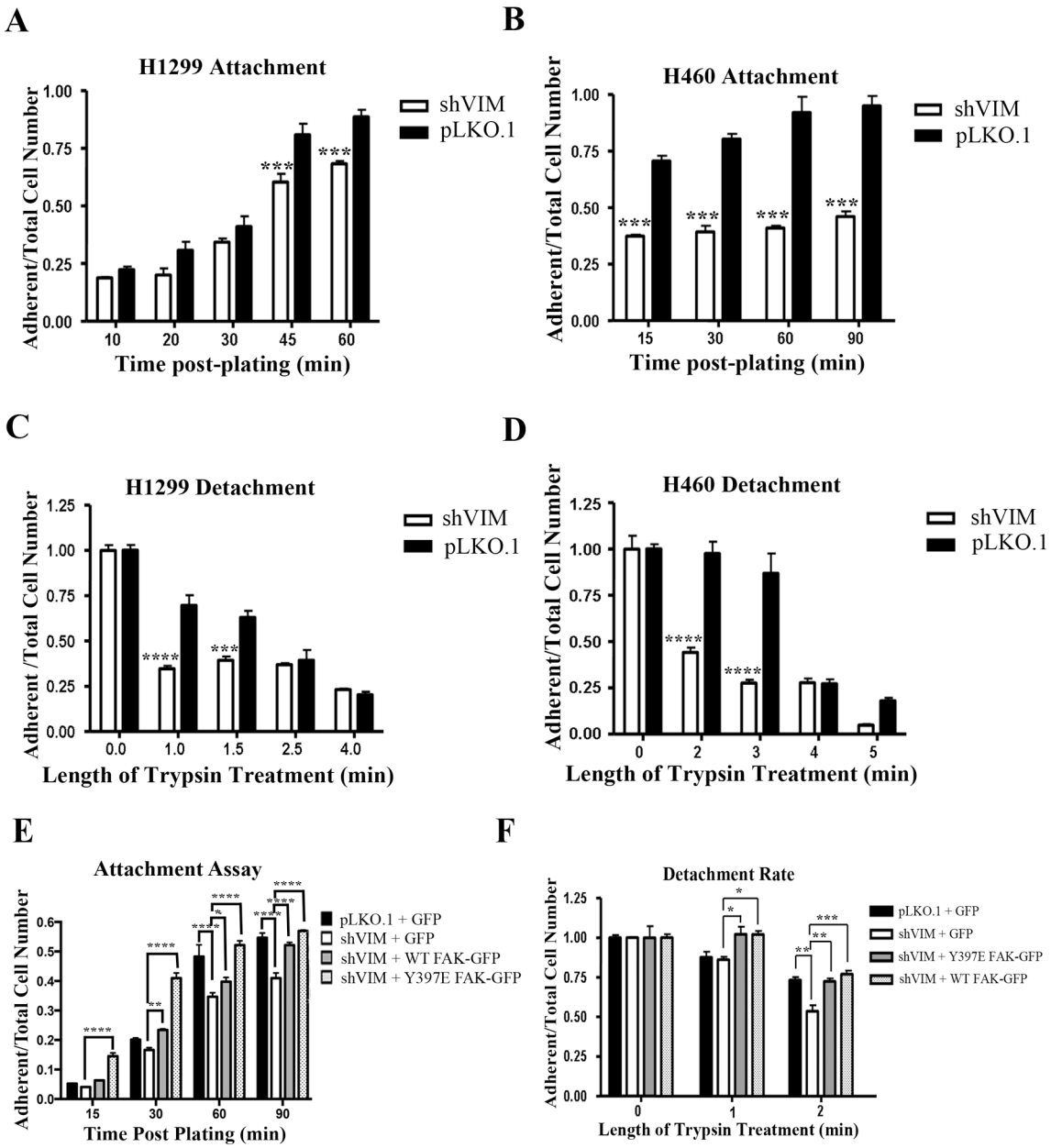


**Figure 5. Vimentin regulates FAK-mediated cell adhesion**

(A–B) H1299 (A) or H460 (B) shVIM and pLKO.1 cells were plated on fibronectin over time. The ratio of adherent to total cells plated was calculated for each cell type at each time point. Both shVIM cell lines attached more slowly than the pLKO.1 cells. *** $p < 0.001$ (C–D) The detachment rate of H1299 (C) or H460 (D) shVIM and pLKO.1 cells was measured by trypsinizing cells over time. For each time point, the ratio of adherent cells to the total cells was calculated. shVIM cells detached faster than pLKO.1 cells. *** $p < 0.001$, **** $p < 0.0001$. (E) The attachment rate was determined for H1299 pLKO.1 cells transfected with GFP and H1299 shVIM cells transfected with GFP, Y397E FAK-GFP or WT FAK-GFP. Expression of Y397E FAK-GFP or overexpression of WT FAK-GFP rescued the attachment defects seen in GFP transfected shVIM cells. * $p < 0.05$, ** $p < 0.01$, **** $p < 0.0001$ (F)

The detachment rate was determined for H1299 pLKO.1 cells transfected with GFP and H1299 shVIM cells transfected with GFP, Y397E FAK-GFP or WT FAK-GFP. Expression of Y397E FAK-GFP or overexpression of WT FAK-GFP rescued the adhesion defects seen in GFP transfected shVIM cells. * $p < 0.05$, ** $p < 0.01$, *** $p < 0.001$.

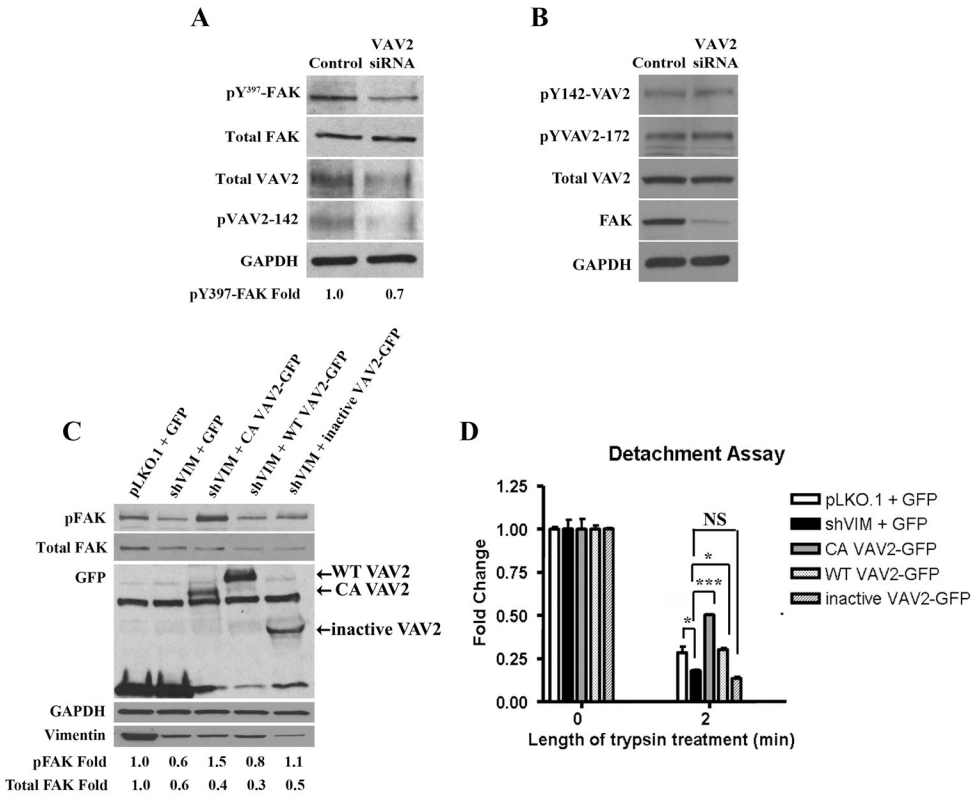


**Figure 6. VAV2 regulates vimentin dependent FAK activation and cell adhesion**

(A) Lysates from H1299 cells transfected with VAV2 or control siRNA were analyzed by Western blotting. pY397-FAK levels were reduced upon VAV2 depletion. A representative western blot out of multiple independent experiments is shown. Fold changes were determined by densitometry. (B) Lysates from H1299 cells transfected with FAK or control siRNA were analyzed by western blotting. There was no change in pY142-VAV2, pY172-VAV2 or total VAV2 levels upon FAK depletion. (C) Western blot of H1299 pLKO.1 cells transfected with GFP and H1299 shVIM cells transfected with GFP, CA VAV2-GFP, WT VAV2 or inactive VAV2 shows that CA VAV2-GFP expression rescued the pY397-FAK defect seen in GFP transfected shVIM cells. A representative western blot out of multiple independent experiments is shown. Fold changes were determined by densitometry. (D) A detachment assay with H1299 pLKO.1 cells transfected with GFP and H1299 shVIM cells transfected with GFP, CA VAV2-GFP, WT VAV2 or inactive VAV2 shows that CA VAV2-GFP but not inactive VAV2-GFP expression rescued the cell adhesion defect seen in GFP transfected shVIM cells. * $p < 0.05$, *** $p < 0.001$.

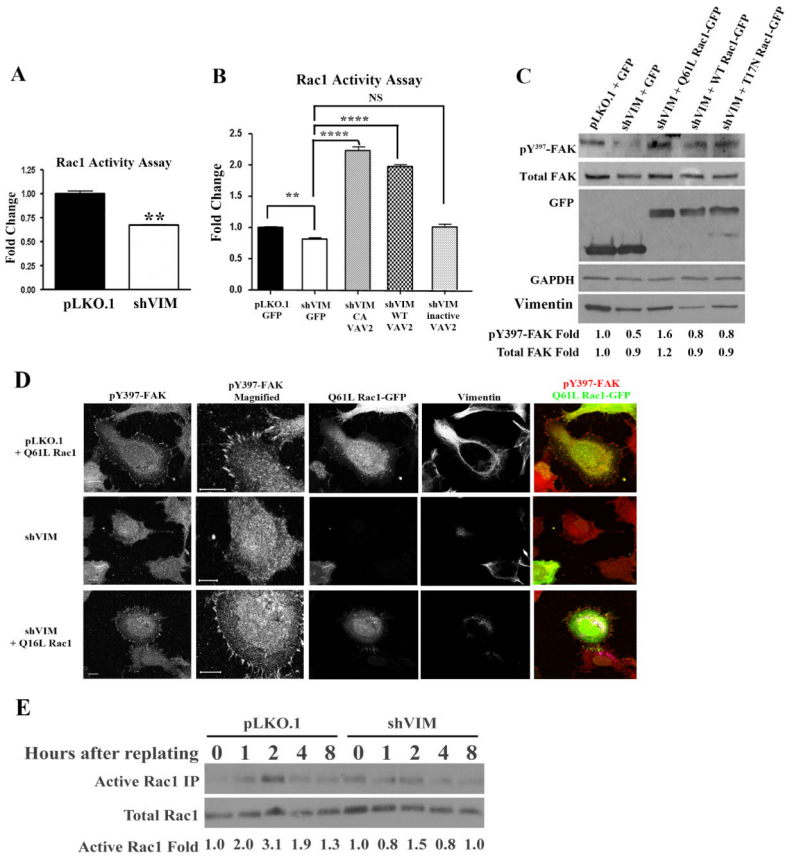


**Figure 7. Vimentin regulates VAV2-mediated Rac1 activation**

(A) An ELISA based Rac1 activation assay showed that Rac1 activity was reduced in shVIM cells compared to pLKO.1 cells. ** $p < 0.01$. (B) H1299 pLKO.1 cells were transfected with GFP and shVIM cells were transfected with GFP, CA VAV2-GFP, WT VAV2-GFP or inactive VAV2-GFP. Transfection with CA VAV2-GFP or WT VAV2-GFP but not inactive VAV2-GFP rescued Rac1 activity. ** $p < 0.01$, **** $p < 0.0001$. (C) Western blot of H1299 pLKO.1 cells transfected with GFP and shVIM cells transfected with GFP, Q61L Rac1-GFP, WT Rac1-GFP or T17N Rac1-GFP. Transfection of Q61L Rac1-GFP rescued the FAK activation defect observed in GFP transfected shVIM cells. A representative western blot out of multiple independent experiments is shown. Fold changes were determined by densitometry. (D) A Rac1 activity pull-down assay on serum starved cells that were trypsonized then replated showed that cells expressing vimentin have a higher level of Rac1 activity during cell spreading than those depleted for vimentin. (E) H1299 pLKO.1 and shVIM cells were transfected with Q61L Rac1-GFP. Confocal images show co-staining of Q61L Rac1-GFP (green), pY397-FAK (red) and vimentin (greyscale). Expression of Q61L Rac1 restored FAK-positive focal adhesions in vimentin shRNA cells. Scale bars =10 μm.

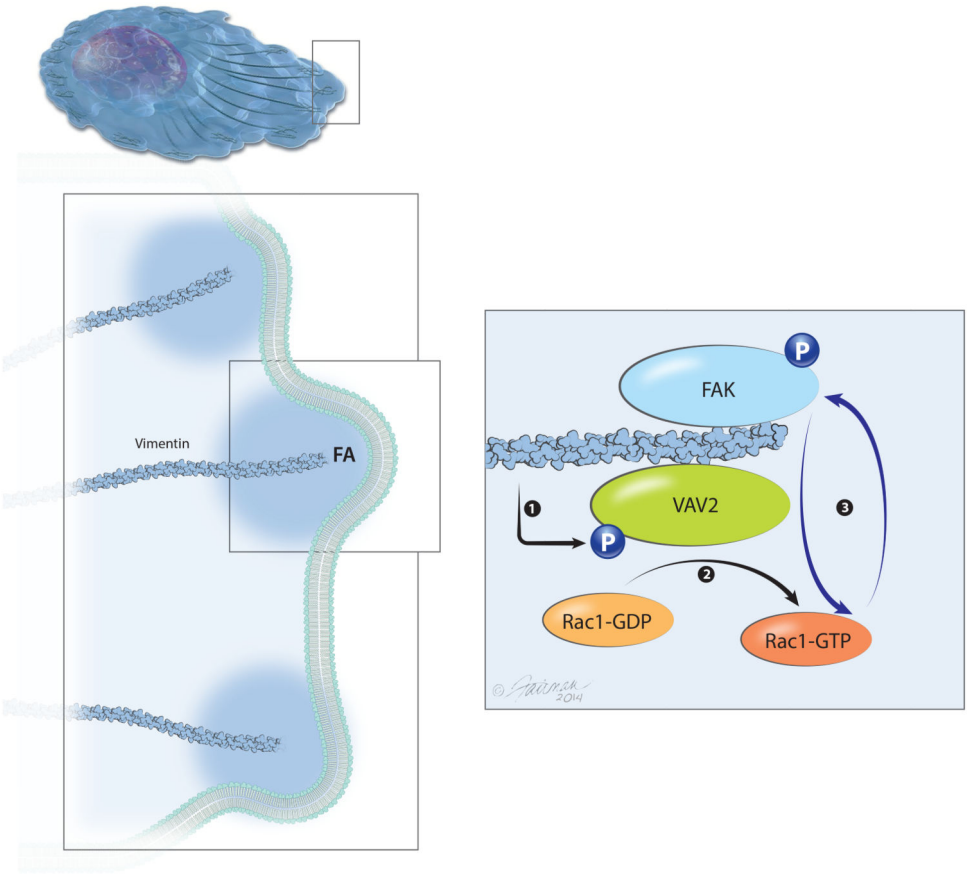


**Figure 8. Vimentin regulates FAK activity through a VAV2-Rac1 dependent pathway**

In the presence of vimentin, VAV2 is phosphorylated at Y142 and localizes to the focal adhesions with FAK and vimentin. Phosphorylated VAV2 activates Rac1, which allows FAK activation at the focal adhesions.